Journal of Applied Mechanics and Technical Physics, Vol. 38, No. 1, 1997

AN EXPERIMENTAL INVESTIGATION OF THE NOZZLE ROUGHNESS EFFECT ON STREAMWISE VORTICES IN A SUPERSONIC JET

V. I. Zapryagaev and A. V. Solotchin

UDC 533.6.011

The supersonic nonisobaric jet structure includes a system of shocks, expansion waves, and mixing layers. It has been found comparatively recently that there is a steady azimuthal nonuniformity in the distribution of gas-dynamic parameters [1, 2] at the boundary of a supersonic axisymmetric jet issuing into ambient space, which is identified with nonuniformity arising in flows with steady streamwise vortices. A three-dimensional structure has also been found in rarefied gas jets [3, 4]. The flow with streamwise vortices in supersonic nonisobaric jets at high Reynolds numbers has also been studied by using, apart from probing measurement methods and schlieren pictures, jet cross-section visualization by means of a laser sheet technique [5, 6].

We associate the generation of three-dimensional peculiarities in the mixing layer of a supersonic jet with Görtler instability, and this is confirmed by the calculations in [7]. The effect of the nozzle inner-surface roughness on the formation of streamwise vortices in a jet is still poorly explored, although some attempts have been undertaken [5]. The considerable difference in the azimuthal distribution of gas-dynamic parameters for the same discharge jet regimes but for different nozzles and different facilities [1, 2, 5, 6, 8] indicates the presence of an uncontrollable parameter that affects the generation and development of streamwise vortex structures. This parameter could be nozzle surface roughness.

The results of an experimental investigation of the effect of artificial microroughness of the nozzle surface on the generation and development of streamwise vortex structures in the initial portion of a high-speed jet are described in the present paper.

1. The experiments were carried out in a jet facility at the Institute of Theoretical and Applied Mechanics, Siberian Division, Russian Academy of Science. The object of study was a high-speed cold-air jet with stagnation temperature $T_0 = 273$ K which was issuing from an axisymmetric nozzle into ambient space at atmospheric pressure P_h and temperature $T_h = 293$ K.

The Reynolds number Re_d was calculated from the nozzle-exit flow parameters and from the nozzle diameter d_a, and the nozzle-exit Mach number M_a was determined from the nozzle geometry. The diameter of the subsonic nozzle entrance d_s, the nozzle length L_a, and the ratio of the nozzle-exit pressure to the ambient pressure P_a/P_h are listed in Table 1.

Sketches of nozzle Nos. 1 and 2 are shown in Fig. 1a and 1b, respectively. Supersonic nozzle No. 1 with exit diameter $d_a = 20$ mm and length $L_a = 90$ mm was mounted in an adapter 2, whose length was $L_1 = 67$ mm (Fig. 1a). The half-angle of the conical (supersonic) part of the nozzle was 8°. The nozzle was attached to a rotating device 3 used to rotate the nozzle at a constant angular velocity equal to one round per 60 sec. Insertion 4 was fixed on the upper cover of a plenum chamber 5 with inside diameter 330 mm. The nozzle profile No. 2 (Fig. 1b) was designed in accordance with Vitoshinskii's formula. The length of the cylindrical (subsonic) part of the nozzle was $\Delta L = 250$ mm.

Institute of Theoretical and Applied Mechanics, Siberian Division, Russian Academy of Sciences, Novosibirsk 630090. Translated from Prikladnaya Mekhanika i Tekhnicheskaya Fizika, Vol. 38, No. 1, pp. 86–96, January–February, 1997. Original article submitted February 15, 1995; revision submitted October 11, 1995.

 0021-8944/97/3801-0078 $18.00

TABLE 1

Nozzle	L_a	d_a	d_s	Re_d	P_a/P_h	M_a
	mm					
No. 1	90.0	20.0	42.0	$5.05 \cdot 10^6$	4.12	1.5
No. 2	105	40.0	87.0	$1.58 \cdot 10^6$	1.0–2.0	1.0

The spatial nonuniformity in the jet was found to be "attached" to the nozzle surface. Therefore, azimuthal displacement of the jet relative to the total-pressure pickup was accomplished by rotation of the nozzle around its axis. The total-pressure pickup (the Pitot tube) with outside diameter 0.6 mm was attached to a traverse gear fabricated on the basis of a microscrew and a step motor. The traverse gear ensured displacement of the pressure pickup along the radius and along the jet axis with an accuracy of 0.05 and 0.1 mm, respectively. The nozzle (including its subsonic part) was rotated at a constant angular velocity. The signal from the total-pressure pickup P_0 was supplied to an XY recorder. This scheme allowed us to study the total-pressure variation versus both the jet radius r and the azimuthal angle φ. The Pitot-tube position was determined by the x and r coordinates, and by the slope of the velocity vector to the jet axis. The latter was found using the available ideas of the flow field and schlieren pictures. The pressure P_t in the receiver of the jet facility was kept constant within 2%. The measurements were performed at different distances from the nozzle exit cross section (x/r_a = 1–4, where $r_a = d_a/2$).

The radial velocity profile in the immediate vicinity of the nozzle exit ($x/r_a = 0.015$) was measured by a flat total pressure pickup with external dimensions 0.2 × 1.2 mm. The jet pressure P_0 or P_0' and the plenum-chamber pressure P_t was measured by inductive gages, which were calibrated both prior to and after the experiment. The plenum-chamber temperature T_t was measured by a resistance thermometer. A data acquisition system based on a CAMAC crate-controller connected to a personal computer was used for the measurements.

When studying the effect of roughnesses of the internal surface of the nozzle on the generation and development of vortex structures in a jet mixing layer, one should know the nozzle-exit boundary-layer characteristics. The calculation of a compressible nozzle flow with a streamwise pressure gradient is a nontrivial problem; therefore, we shall use approximate estimates, which will be compared with the measured results.

For gradient-free laminar flow, the Reynolds number Re_{δ^*} calculated from the external-flow parameters and displacement thickness, at 0 < M < 5, can be evaluated with an accuracy of 5% by the formula of [9]:

$$\mathrm{Re}_{\delta^*} = 1.73(1 + 0.5(\gamma - 1)\,\mathrm{M}^2)\sqrt{\mathrm{Re}_x}. \tag{1.1}$$

Here Re_x is the Reynolds number calculated for length x. Assuming the nozzle length $x = L_a + \Delta L$ to be the reference length, we obtain an expression for estimating the displacement thickness:

$$\delta^* = 1.73(1 + 0.5(\gamma - 1)\mathrm{M}^2)\sqrt{Ld/\mathrm{Re}_d}. \tag{1.2}$$

The estimates yield $\delta^* = 0.05$ and 0.13 mm for nozzle Nos. 1 and 2 ($\mathrm{Re}_d = 1.06 \cdot 10^6$), respectively.

Figure 2 shows the velocity profile (points 1) of the mixing layer of a subsonic flow measured near the exit of nozzle 2 at a distance of $x = 0.015r_a$ (r_a is the nozzle diameter). The plenum-chamber pressure was P_t = 165 kPa, and $\mathrm{Re}_d = 1.06 \cdot 10^6$. The normalized velocity u/U_a calculated from the measured pressure P_0 (U_a is the jet velocity at the nozzle exit) is plotted on the abscissa. The dimensionless radial coordinate is (as in [10]) $\eta = r\sqrt{U_a/\nu_a L_e}$. Here ν_a is the kinematic viscosity at the nozzle exit, and L_e = 153 mm is the reference longitudinal length ($L_a < L_e < L_a + \Delta L$). This value of L_e was adopted from the condition of coincidence of the measured velocity profile with the Blasius profile for a certain value of the radius for which $u/U_a = 0.5$. For comparison, Fig. 2 shows profiles of the form $u/U_a = (r/\delta)^m$ for $m = 1/7$ and $1/9$, corresponding to the turbulent flow regime (curves 3 and 4). One can see that the measured velocity profile is in good agreement with the Blasius profile (curve 2). The adopted value of L_e is larger than the nozzle length but smaller than $L_a + \Delta L$, which is caused by both the gradient flow and the axisymmetric pattern.

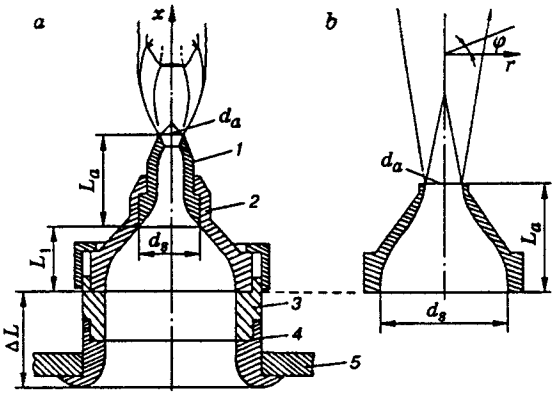

Fig. 1

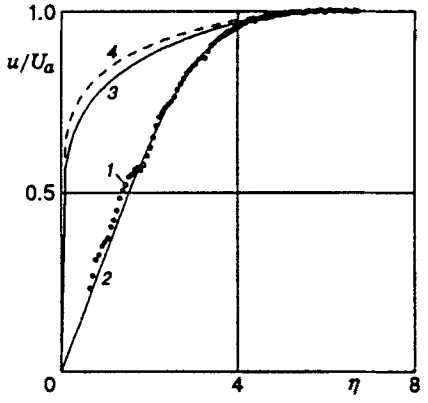

Fig. 2

Two conclusions can be drawn from analysis of the results presented in Fig. 2. First, the flow in a convergent nozzle for $d_a = 40$ mm and $\mathrm{Re}_d \sim 10^6$ is laminar. In our opinion, this is important, since it is known [11] that the laminar-turbulent transition for a nozzle with $d_a = 50$ mm occurs at $\mathrm{Re}_d = 10^4$. Second, the use of simple relations for a flat plate ignoring the gradient allowed one to obtain a satisfactory agreement of estimates for the laminar boundary-layer thickness in the nozzle. The latter factor is noted in [12] in estimation of the boundary-layer parameters for hypersonic nozzles. Extrapolating the measured velocity profile for the jet issuing from nozzle No. 2, one can assume that a laminar flow regime at the nozzle exit is realized for nozzle No. 1 at $\mathrm{Re}_d = 4.1 \cdot 10^6$. This is supported by a set of experimental data on the laminar-turbulent transition in wind tunnels, according to which for sharp cones at M = 1.5, the transition Reynolds numbers are $\mathrm{Re}_t = (3\text{–}7)\cdot 10^6$ [13, 14]. In this case, a nonseparated flow inside the nozzle is formed at a negative pressure gradient, which has a stabilizing effect on the development of Tollmien–Schlichting disturbances, which, in turn, increases the transition Reynolds numbers, as compared with those for a gradient-free flow [10].

2. The nozzle surface roughness size was chosen by Dryden's criterion [9, 15], according to which the roughness has a substantial effect on the transition Reynolds number at $\mathrm{Re}_k = (U_\infty k)/\nu_\infty$, where k is the roughness size. This relation shows that the influence on the boundary-layer characteristics is effective when $k \sim \delta^*$.

In the present experiments, the roughness of nozzle No. 1 was of three different types: one natural — instrumental roughness (below, simply natural) with individual elements not larger than 0.002 mm — and two artificial types of roughness, i.e., in the form of longitudinal scratches with a depth of about 0.05 mm, whose step and positions were varied, and in the form of sand roughness with a grain size of 0.05–0.08 mm. The grains were glued onto certain parts of the surface. The grain sizes and positions on the inner surface of the nozzle were measured from photomicrographs obtained using a microscope. Thus, the normalized roughness size was $k/\delta^* \sim 0.04$ and ~ 1 for natural and artificial types of roughness, respectively. The schlieren technique was used for visualization of the supersonic underexpanded flow pattern.

Figure 3 gives the measured nonuniformity of the total pressure distribution $P_0'(\varphi)$ versus the azimuthal angle φ for different types of roughness on the internal surface of nozzle No. 1. The experimental data correspond to a distance of $x/r_a = 2.0$ between the probe and the nozzle exit. Curve 1 is characteristic of a nozzle whose internal surface had scratches 0.05 mm deep with a step of 1 and 2°. The scratches were made at different sections of the internal surface of the nozzle: at subsonic and supersonic sections, at the throat section, at the butt-end of the nozzle, and one segment of the nozzle had natural roughness (control surface). The entire circumference of the nozzle cross section was split into five equal segments of 72°. Curve 2 corresponds to sand roughness applied to the throat section within the range $\varphi = 0\text{–}180°$ ($\varphi = 180\text{–}360°$ is the region with natural roughness). The size of the particles glued onto the surface was (0.08 ± 0.02) mm in this case, and they were calibrated by passing through two sieves. The particles were glued in one layer as a

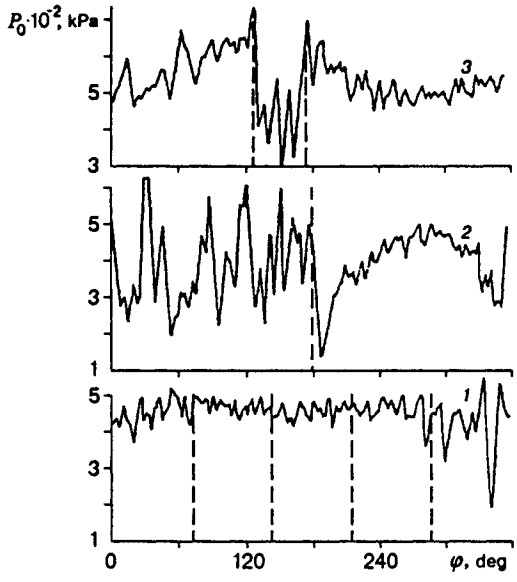

Fig. 3

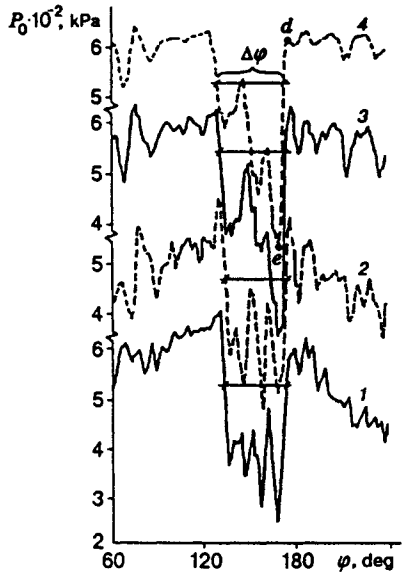

Fig. 4

band 1 mm wide. Curve 3 refers to smaller particles with a transverse size of 0.05 mm which were glued onto the internal surface near the nozzle exit within the range of azimuthal angles $\varphi = 130$–$180°$.

Comparison of the curves of pressure P_0' versus the angle φ (with artificial roughness) with similar curves for natural nozzle roughness [1, 2, 5–8] shows that the amplitude of variation of the total pressure is increased by additional roughness. A stronger effect of sand roughness on the amplitude of the total-pressure variation is observed, as compared with scratches in the nozzle (it will suffice to compare curve 1 with curves 2 and 3).

The amplitude of the total-pressure variation for curve 1 is comparable with the amplitude of variation of the total pressure P_0' corresponding to sections with natural roughness of curves 2 and 3. The roughness at the throat section increases the amplitude of variation of P_0', and this is explained by the larger grain size. Curve 3 clearly shows a nonuniform distribution of the total pressure within the range $\varphi = 130$–$180°$, which corresponds to the sand roughness.

When analyzing the results of Fig. 3, one should note that the amplitude of variation of the total pressure increases when the flow passes over the nozzle surface with larger roughness. In this case, one can speak about an increase in vortex intensity, which is indirectly determined by the maximum and minimum deviations of the total pressure from the average level. Along with the increase in the amplitude of the total-pressure variation, a decrease in the averaged measured pressure $\langle P_0'(\varphi)\rangle$ is observed. Here the angle brackets indicate averaging over φ. The decrease in $\langle P_0'\rangle$ is most probably caused by intensification of mixing and by an increase in the mixing-layer thickness in the jet regions corresponding to artificial nozzle roughness.

Figure 4 shows the total pressure versus the azimuthal angle for the third case, where the roughness is applied within the range $\varphi = 130$–$180°$ for $x = x/r_a = 1$, 2, 3, and 4. The curve of $\langle P_0'(\varphi)\rangle$ has a "canyon," which corresponds to the range of angles where the roughness is applied. Another important result of the study is the small range of propagation of the disturbances caused by the roughness in the mixing layer of a supersonic jet.

For the chosen gas-dynamic jet parameters, the width of the "canyon" with respect to the azimuth $\Delta\varphi$, defined by the angular distance measured at $P_0' = (P_{0e}' + P_{0d}')/2$ in cross sections $x/r_a = 1$, 2, 3, and 4, changes only slightly and corresponds to $\Delta\varphi = 40$, 40, 43, and 45°. The latter is indicative of small propagation velocities of disturbances such as streamwise vortex structures in the azimuthal direction. In Fig. 4, $P_{0d}' = \langle P_0'(\varphi)\rangle$ for $\varphi = 0$–$130°$ and $\varphi = 180$–$360°$ corresponds to the averaged pressure for natural

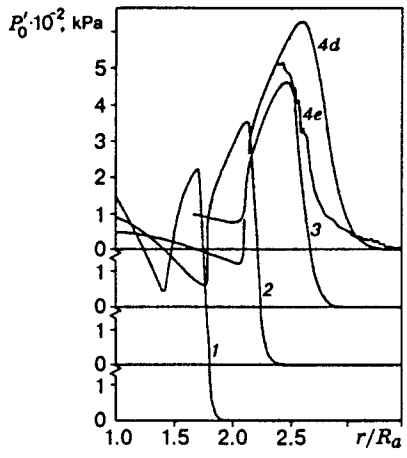

Fig. 5

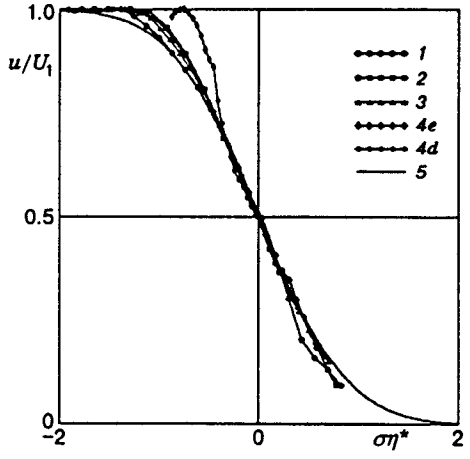

Fig. 6

conditions, and $P'_{0e} = \langle P'_0(\varphi) \rangle$ for $\varphi = 130$–$180°$ corresponds to the averaged pressure in the region with roughness.

The radial total-pressure distribution profiles $P'_0(r)$ for $x/r_a = 1$, 2, 3, and 4 (curves 1–4) are presented in Fig. 5. Profiles 1–3 were obtained for $\varphi = 0$. Profile 4d corresponds to the comparatively undisturbed state of the nozzle surface, and profile 4e corresponds to the sand roughness (profiles 4d and 4e were obtained for angles φ that are equal to φ_d and φ_e in profile 4 of Fig. 4). The character of the total-pressure variation along the jet radius depends on the value of φ, as was noted in [8]. In this case, the large amplitude of variation of $P'_0(\varphi)$ shows that streamwise vortices occur in a region in which $dU/dr < 0$. This is caused by the high intensity of the vortices generated by the artificial roughness. As a result of this, a high-pressure flow is removed from the inviscid compressed layer and a low-pressure gas from the jet periphery is entrained in the compressed layer.

The results presented show that the nozzle-surface roughness exerts a significant effect on the generation and development of streamwise vortex structures in the mixing layer of the initial region of a supersonic jet.

The flow-velocity distribution in the corresponding cross sections of the jet mixing layer was determined from the measured static and total pressures (Fig. 5). Figure 6 plots the dimensionless velocity u/U_1 as a function of the coordinate $\sigma\eta^*$, where $\eta^* = (r - r_{0.5})/x$, $\sigma = \pi/\delta_\eta$ is the divergence parameter, and δ_η is the shear-layer thickness calculated from the slope of the velocity profile versus η^* [12]. The velocity U_1 corresponds to the maximum total pressure for the profiles in Fig. 5, and it is attained at a radial distance $r = r_1$. The static pressures measured in various jet cross sections show that the static pressure in the jet for $r > r_1$ differs from atmospheric pressure for the flow regimes studied by not more than 1%. The velocity was calculated from isentropic-flow formulas with allowance for the total-pressure losses in the normal shock at M > 1. Taking into account that the difference of jet stagnation temperature T_t from the ambient temperature T_h does not exceed 10%, we assume a linear temperature variation from T_h to T_t versus the radius.

It follows from Fig. 6 that the measured velocity profiles (except for profile 4e) are satisfactorily described by the error function

$$u/U_1 = [1 - \mathrm{erf}(\sigma\eta^*)]/2. \tag{2.1}$$

Profiles 1–4e, and 4d in Fig. 6 are calculated from the total-pressure profiles in Fig. 5, and profile 5 is calculated by formula (2.1). The measured values of δ_η and σ are presented in Table 2.

3. The above results describe the effect of the internal-surface roughness of a supersonic nozzle on the generation and development of disturbances in the jet shear layer. The results of similar experiments for the mixing layer of the jet issuing from a convergent nozzle at flow Mach numbers both higher and lower than unity are also of interest. For this, the internal surface of nozzle No. 2 was covered by one layer of spherical

TABLE 2

Number of profile (Fig. 6)	x/r_a	δ_η	σ
1	1	0.148	11.9
2	2	0.103	17.2
3	3	0.129	13.7
4e	4	0.342	5.2
4d	4	0.144	12.3

TABLE 3

Number of regime	P_t, kPa	M_j	$Re_d \cdot 10^6$	δ^*, mm
1	142	0.726	0.83	1.80
2	160	0.848	1.02	1.60
3	180	0.956	1.2	1.50
4	200	1.046	1.35	1.40
5	300	1.358	2.02	1.10

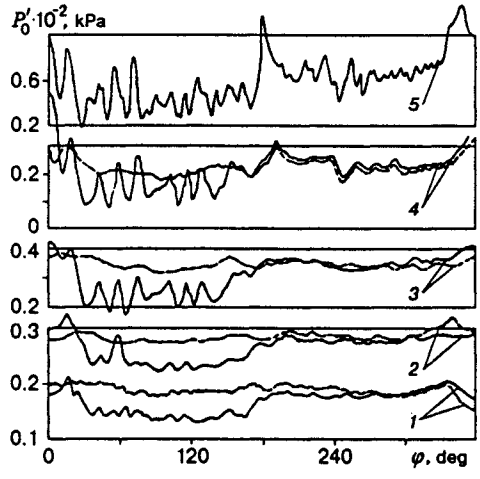

Fig. 7

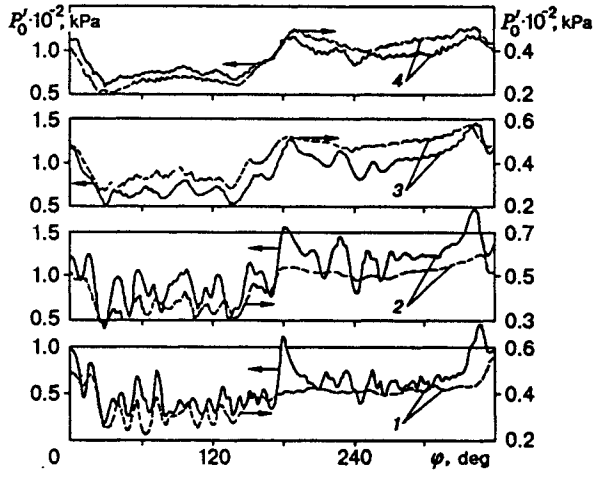

Fig. 8

particles 0.05 mm in diameter. The particles were glued near the nozzle-exit cross section as a 1-mm-wide strip on half of the circumference length $\varphi = 0$–$180°$. The thickness of the varnish film did not exceed several micrometers.

Curves 1–5 in Fig. 7 show the total pressure versus the azimuthal angle for five regimes whose parameters are listed in Table 3. The results were obtained for the jet cross section $x/r_a = 1.0$. The data for this cross section were found at a radial distance from the jet axis at which the total-pressure variations are maximal. The mean total pressure equal to $\langle P_0'(r) \rangle = 0.5 P_0'(r_1)$ is established at distance $(r_1 + \delta/2)$.

For regime Nos. 1–4, the dashed curves show $P_0'(\varphi)$ without additional roughness (Fig. 7). For $180° < \varphi < 360°$ (natural roughness), there is no difference between azimuthal curves of $P_0'(\varphi)$ with and without additional roughness for $0 < \varphi < 180°$. This indicates that the disturbed portion of the shear layer has little effect on the undisturbed part, and this can be attributed to the convective propagation of the disturbances generated by the nozzle roughness. One can see from Fig. 7 that the amplitude of the nonuniform jet pressure distribution increases for the azimuthal angles corresponding to the nozzle roughness. The mean pressure value decreases, and this can be attributed to intensification of the mixing process in this portion of the mixing layer. The presence of additional roughness in the nozzle has a weak effect on the formation of nonuniform azimuthal distributions of gas-dynamic quantities for regime No. 1, but this effect becomes significant with a rise in the plenum-chamber pressure.

For a supersonic jet (regime No. 5), the nonuniformity of the azimuthal total-pressure distribution within the range of $180° < \varphi < 360°$ is virtually similar to the nonuniformity caused by sand roughness within $0 < \varphi < 180°$.

Figure 8 plots curves of $P_0'(\varphi)$ that characterize the streamwise propagation of the azimuthal pressure

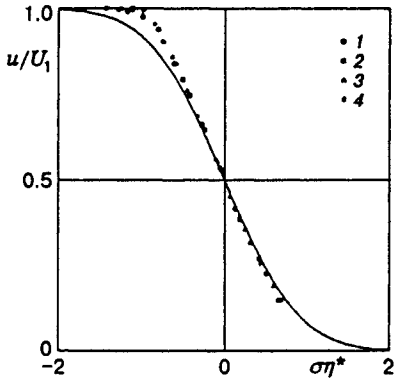

Fig. 9

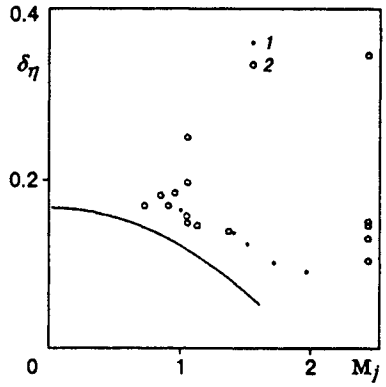

Fig. 10

nonuniformity for regime Nos. 1 and 5 (Table 3), which correspond to nozzle-exit isentropic Mach numbers $M_j = 0.73$ and 1.36 (dashed and solid curves, respectively). The curves are obtained for $x/r_a = 1$, 2, 3, and 4 (curves *1–4*). The rapid damping of the azimuthal nonuniformities of the total-pressure distribution in the mixing layer at $M_j < 1$ and their increase at $M_j > 1$ should be noted. This is caused by a sudden change in the streamline curvature at the jet boundary near the convergent nozzle exit section, which is due to additional flow deflection in the expansion wave at $M_j > 1$. At $M_j < 1$, the streamlines in the shear layer near the nozzle exit section have a small curvature and, at $M_j > 1$, the curvature radius has a finite value, and it can be determined from the formula [16] $R = \sqrt{(M_j - 1)/\sin(\theta_H)}$. The angle θ_H is determined by the nozzle geometry and by the Mach number at the jet boundary. This angle corresponds to the flow-deflection angle in the centered expansion wave, $\theta_H = \theta_a + H(M_j) - H(M_a)$, where $H(M)$ is the Prandtl–Mayer function. In our case, $\theta_a = 0$ and $H(M_a) = 0$ for $M_a = 1$.

4. Figure 9 shows velocity profiles for the convergent-nozzle flow regimes examined. Experimental points 1–4 are obtained for regime No. 3 (Table 3) and refer to the cross sections $x/r_a = 1$, 2, 3, and 4. An affine similarity of velocity profiles for different cross sections is observed. The graph also includes the curve of (2.1), which describes a developed mixing layer at large distances from the nozzle exit. Some difference of the measured velocity values from the approximating functions indicates, most probably, a transition flow the initial region of the jet.

The shear-layer thickness δ versus the flow Mach number at the jet boundary M_j is presented in Fig. 10, where curve 2 is determined by the relation $\delta_\eta = 0.165 - 0.045M_j$, which is a good approximation of the results of measurements using a laser-Doppler anemometer. Points 1 are the results of measurements using a total-pressure probe in [12]. Our data (points 2) for $M_j < 1.4$ (a convergent nozzle at $M_a = 1$) characterize the averaged thickness of the mixing layer, averaging being performed over four cross sections of the jet ($x/r_a = 1$, 2, 3, and 4).

The effect of the azimuthal nonuniformity of distributions of gas-dynamic parameters on the shear layer thickness is determined for the flow issuing from a supersonic nozzle at $M_a = 1.5$ or for a jet at $M_j = 2.4$. For this, the graph includes nonaveraged values of δ_η corresponding to the total-pressure profiles $P_0'(r)$ in Fig. 5. The outside point ($\delta_\eta = 0.34$) refers to a radial total-pressure profile (profile 4e in Fig. 5) that was obtained at a local minimum of the curve of $P_0'(\varphi)$ (point e in Fig. 4). Several values at $M_j = 1.05$ illustrate the azimuthal-nonuniformity effect at $x/r_a = 1.0$. Thus, we can state that the velocity profiles in the mixing layer are satisfactorily represented by the error function (2.1), except in those regions of the mixing layer in which the local minimum of $P_0'(\varphi)$ is observed. Comparison of the measured values of the mixing-layer thickness with the data of [12] shows their agreement if there is no additional nozzle roughness.

It is clear from the results obtained that when studying the mixing layer in the initial region of a supersonic jet, one should take into account the nozzle-flow character. Using the available numerical data for Görtler instability [17, 18], we can suggest the following scheme of generation and development of steady

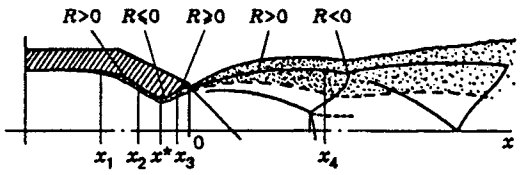

Fig. 11

disturbances caused by the curvature of streamlines. The disturbances of the Taylor–Görtler type are known to increase with a positive curvature of streamlines if $dU/dn < 0$ (n is the normal direction to the streamline).

Figure 11 shows typical regions inside and outside the nozzle in which the curvature of streamlines can change sign. The derivative of the velocity normal to streamlines is a negative quantity both in the boundary layer and in the mixing layer. At $x_1 < x < x_2$, where the cylindrical-nozzle contour with $R = 0$ becomes conical, the subsonic flow is accelerated along the concave wall with a positive curvature ($R > 0$). Görtler-type disturbances will increase in this flow region. At the nozzle throat cross section, the flow past a convex wall occurs which can attenuate this type of disturbances. The cross section x_3 corresponds to a point on the supersonic portion of the nozzle section. Downstream of this point there is flow along the surface with a positive curvature. Under certain conditions, even a small curvature of the supersonic part of the nozzle can cause substantial growth of Görtler-type disturbances up to flow turbulization [19].

It should be noted that the surface curvature in the region $x_3 < x < 0$ can be equal to zero, for example, in conical nozzles. When a supersonic underexpanded jet is issuing from a conical nozzle (with zero curvature behind the cross section x_3), there is nearly always a flow region with a positive curvature of streamlines at its boundary (see Sec. 3). In this case, the value and sign of the curvature of streamlines in the shear layer of the jet can also be changed in the cross section $x = 0$. Finally, the curvature of streamlines at the jet boundary changes at the end of the initial section (cross section x_4). All these features that characterize the nozzle flow and jet can lead to either strengthening or attenuation of Görtler-type disturbances.

5. The high receptivity of the azimuthal distribution of gasdynamic parameters to the condition of the internal nozzle surface can be caused by the laminar-turbulent transition in the initial region of the high-speed jet with a laminar discharge from the nozzle exit. The hypothesis that there are two mechanisms of laminar-turbulent transition in the mixing layer of a rarefied jet was proposed by S. A. Novopashin as applied to the observed regime of flow self-organization in a supersonic jet at $\mathrm{Re}_d \sim 10^4$–10^5. Under the conditions considered in the present paper ($\mathrm{Re}_d = 10^6$), where the laminar character of the flow at the nozzle exit was experimentally verified, it seems possible that disturbances can develop in the mixing layer owing to both Kelvin–Helmholtz instability and Taylor–Görtler instability with subsequent flow turbulization.

In conclusion, the study performed showed that the roughness of the internal nozzle surface plays a substantial role in the formation and development of streamwise vortex structures in the initial region of a supersonic jet. The intensity, transverse size, and extent of the vortex structures, in turn, depend on the geometric shape and size of the microroughness and on their position in the nozzle. The measurements in the shear layer in the immediate vicinity of the nozzle indicate a laminar flow character in the nozzle boundary layer at $\mathrm{Re}_d \sim 10^6$, which is consistent with experimental data on the laminar-turbulent transition in wind tunnels. The shear-layer thickness measured by the Pitot tube is shown to agree with the results of [20] for transonic discharge velocities. Analysis of the nozzle-boundary-layer flow and of the mixing-layer flow in the initial region of the jet, as applied to the shear-flow stability against Görtler disturbances, indicates the existence of at least three regions in which disturbances of this type can strengthen. These are the sub- and supersonic portions of a nozzle and the initial region (the first cell) of a supersonic underexpanded jet.

REFERENCES

1. V. I. Zapryagaev and A. V. Solotchin, "Spatial structure of flow in the initial section of a supersonic underexpanded jet," Preprint No. 23-88, Inst. Theor. Appl. Mech., Sib. Div., USSR Acad. Sci., Novosibirsk (1988).
2. V. I. Zapryagaev and A. V. Solotchin, "Three-dimensional flow structure in a supersonic underexpanded jet," *Prikl. Mekh. Tekh. Fiz.*, No. 4, 42–47 (1991).
3. S. A. Novopashin and A. L. Perepelkin, "Flow self-organization in a supersonic preturbulent jet," Preprint No. 175, Inst. Thermal Phys., Sib. Div., USSR Acad. Sci., Novosibirsk (1988).
4. K. Teshima, "Three-dimensional characteristics of supersonic jets," *Proc. 17th Conf. on Rarefied Gas Dynamics*, BRD, Aachen (1990), pp. 1042–1048.
5. A. Krothapalli, G. Buzuna, and L. Lourenco, "Streamwise vortices in an underexpanded axisymmetric jet," *Phys. Fluids A*, **3**, No. 8, 1848–1851 (1991).
6. S. A. Arnette, M. Samimy, and G. S. Elliott, "On streamwise vortices in high Reynolds number supersonic axisymmetric jets," *Phys. Fluids A*, **5**, No. 1, 187–202 (1993).
7. N. A. Zheltukhin, V. I. Zapryagaev, A. V. Solotchin, and N. M. Terekhova, "Spectral composition and structure of stationary vortex Taylor–Görtler disturbances in a supersonic underexpanded jet," *Dokl. Ross. Akad. Nauk*, **325**, No. 6, 1133–1137 (1992).
8. V. I. Zapryagaev, S. G. Mironov, and A. V. Solotchin, "Spectral composition of the wavenumbers of longitudinal vortices and characteristics of flow structure in a supersonic jet," *Prikl. Mekh. Tekh. Fiz.*, **34**, No. 5, 41–47 (1993).
9. E. R. van Driest and C. B. Blumer, "Boundary-layer at supersonic speeds–three-dimensional roughness effects (spheres)," *J. Aerosp. Sci.*, **29**, No. 8, 909–916 (1962).
10. G. Schlichting, *Boundary Layer Theory*, McGraw-Hill, New York (1968).
11. A. N. Sekundov and O. V. Yakovlevskii, "Some problems of transition of channel flow to jet flow," *Izv. Akad. Nauk SSSR, Mekh. Zhidk. Gaza*, No. 3, 150–154 (1967).
12. I. I. Mezhirov, "A study of flows in hypersonic nozzles of wind tunnels," *Tr. TsAGI*, No. 2119, Moscow (1981).
13. S. A. Gaponov and A. A. Maslov, *Development of Disturbances in Compressible Flows* [in Russian], Nauka, Novosibirsk (1980).
14. M. R. Malik, "Prediction and control of transition in supersonic and hypersonic boundary layers," *AIAA J.*, **27**, No. 11, 1487–1493 (1989).
15. A. S. Skuratov, A. V. Fedorov, and A. I. Plotskii, "Effect of surface roughness on the laminar-turbulent transition of a boundary layer," in: *Review of the Department of Scientific and Engineering Information of the Central Aerohydrodynamic Institute* [in Russian] (1992).
16. V. G. Dulov and G. A. Luk'yanov, *Gas Dynamics of Discharge Processes* [in Russian], Nauka, Novosibirsk (1984).
17. J. M. Floryan, "On the Görtler instability of boundary layers," *Prog. Aerosp. Sci.*, **28**, 235–271 (1991).
18. J. M. Floryan and W. S. Saric, "Wavelength selection and Görtler vortices," *AIAA J.*, **22**, No. 11, 1529–1538 (1984).
19. I. E. Beckwith, M. R. Malic, F.-J. Chen, and D. M. Bushnell, "Effects of nozzle design parameters on the extent of quiet test flow at Mach 3.5," in: *Laminar-Turbulent Transition*, Springer-Verlag, Berlin (1984), pp. 589–600.
20. J. C. Lau, P. J. Morris, and M. J. Fisher, "Measurements in subsonic and supersonic free jets using a laser velocimeter," *J. Fluid Mech.*, **93**, 1–27 (1979).